Int. J. Solids Structures, Vol. 11, pp. 403–423. Pergamon Press 1975. Printed in Great Britain

BOUNDS FOR FINITE DEFLECTIONS OF IMPULSIVELY LOADED STRUCTURES WITH TIME-DEPENDENT PLASTIC BEHAVIOR†

P. S. SYMONDS‡ and C. T. CHON§

Division of Engineering, Brown University, Providence, R. I. 02912, U.S.A.

(*Received* 2 *January* 1974)

Abstract—The paper shows that upper bounds on deflections of an impulsively loaded structure whose behavior in the plastic range is strain rate dependent may be obtained by an application of the theorem of minimum potential energy, with results valid for finite deflections and strains. The concepts of extremal path behavior in strain–time space, due to Ponter, are used in order to provide unique definitions of strain energy and complementary energy for the path dependent material. The theorems are illustrated by examples of fully constrained beams in which deflections of the order of the beam thickness lead to large forces of membrane type.

1. INTRODUCTION

Upper bounds on deflections and lower bounds on time of deformation (where appropriate) have been obtained by Martin for a variety of elastic and plastic (time-independent) behaviors [2–6]. A class of time dependent inelastic behavior was treated by Martin [7] on the basis of the inequality [8]

$$\dot{q}_j^a Q_j^b \leq w(\dot{q}_j^a) + \Psi(Q_j^b) \tag{1}$$

where Q_j^b, $j = 1,2 .. N$, denotes a particular generalized stress vector at a point in a structure, $\dot{q}_j^a$ is a particular generalized strain rate vector (defined as "corresponding" to generalized stresses Q_j), and the functions w, Ψ are

$$w(\dot{q}_j^a) = \int_0^{\dot{q}_j^a} Q_j \,\mathrm{d}\dot{q}_j; \quad \Psi(Q_j^b) = \int_0^{Q_j^b} \dot{q}_j \,\mathrm{d}Q_j. \tag{2}$$

The material behavior is of general viscous type with $Q_j = Q_j(\dot{q}_k)$, $\dot{q}_j = \dot{q}_j(Q_k)$; these relations between stress and strain rate states being path independent in the spaces respectively of strain rate and stress. Equation (1) describes inelastic behavior obeying Drucker's extended postulates [9, 10] for time dependent inelasticity. By means of the equation of virtual work rate Martin [7] derived an inequality furnishing upper bounds on final deflections in terms of the initial kinetic energy of the impulsively loaded structure. A second inequalitity furnished a lower bound on the duration time from the known initial velocity distribution over the structure. For these bounds Martin made use of the theorem of virtual work rate for infinitesimal deflections, in which the dynamically admissible stress–acceleration system and the kinematically admissible velocity–strain rate fields

†Research reported here was supported by Contract N00014-67-A-0191-0003 of Brown University with Office of Naval Research.

‡Professor of Engineering, Brown University, Providence, R.I. 02912.

§Research Assistant, Division of Engineering, Brown University, Providence, R.I. 02912.

are independent. The resulting limitation to problems of sufficiently small deflections is a serious defect in many potential applications, for example those of beams and plates in which large membrane forces are induced at deflections of the order of the thickness.

The present approach does not make use of the theorem of virtual work rate, nor does it restrict material behavior to the class of viscous behavior treated by Martin. The results are applicable to problems of large deflections and/or strains in an impulsively loaded structure of quite general time dependent inelastic behavior. In the illustrative examples however we consider only problems of fully constrained beams in which membrane forces must be considered when deflections are a few multiples of the beam depth, but may be assumed small compared to overall structural dimensions; and we assume a type of viscous stress–strain rate behavior. The approach makes use of the theorem of minimum potential energy [12], valid for finite deflections, in the spirit of Martin's [5] and Martin and Ponter's [6] derivations of bounds for finite elastic deflections and finite elastic–plastic (time-independent) deflections, respectively.

2. PRESENT APPROACH

"Strain energy" and "complementary strain energy" do not exist as well defined functions of strain and stress, respectively, in a path dependent material. They are however well defined functions of the terminal states if the respective line integrals are computed following *extremal paths*. Following Ponter [1], consider a fixed state of strain q_i^a at a fixed time τ which may be reached by various paths from the origin of a space whose coordinate axes are the strain components $q_1, q_2 \ldots q_N$ and time t. For one or more paths the strain energy is a minimum. We may write

$$\check{W}[q_i^a(\tau)] = \mathrm{ep}\int_0^{q^a(\tau)} Q_i \, \mathrm{d}q_i \leq W[q_i^a(\tau)] = \int_0^{q_i^a(\tau)} Q_i \, \mathrm{d}q_i \tag{3}$$

where the first line integral is marked ep for an extremal path and the second is evaluated following an arbitrary path. (Here $Q_j \, \mathrm{d}q_j$ is the increment of specific work, for example per unit length of a beam, per unit middle surface area of a plate or shell, etc.) Similarly, the complementary strain energy for fixed terminal stress Q_j^b and time τ is maximized by extremal paths in the space (Q_j, t) and we may write

$$\hat{\Omega}[Q_j^b(\tau)] = \mathrm{ep}\int_0^{Q_j^b(\tau)} q_j \, \mathrm{d}Q_j \geq \Omega[Q_j^b(\tau)] = \int_0^{Q_j^b(\tau)} q_j \, \mathrm{d}Q_j. \tag{4}$$

Ponter [1] showed that $\check{W}$ and $\hat{\Omega}$ are convex functions, among other properties. The extremal paths effectively define a material with holonomic properties, the stress becoming a uniquely defined function of strain and time; and vice versa. For the special case of a rate dependent material behavior defined by a homogeneous viscous relation between stress and strain rate the extremal paths (which simultaneously minimize W and maximize Ω) are extremely simple. Thus, if the strain rate is derivable from a function $\Psi[Q_j(\tau)]$ which is homogeneous of degree $n+1$, so that

$$\dot{q}_j[Q_k(\tau)] = \frac{\partial \Psi}{\partial Q_j} \tag{5a}$$

and

$$Q_j\dot{q}_j = Q_j\frac{\partial \Psi}{\partial Q_j} = (n+1)\Psi \tag{5b}$$

(by Euler's theorem), then $W[q_j^a(\tau)]$ is rendered a minimum and $\Omega[Q_j^a(\tau)]$ a maximum if

$$\text{for } 0 < t < \tau, \quad Q_j(t) = \frac{n}{n+1} Q_j^a \tag{6a}$$

$$t = \tau, \quad Q_j(\tau) = Q_j^a. \tag{6b}$$

In other words, for the fixed strain state $q_j^a = (n/n+1)Q_j^a\tau$ attained at time τ, with corresponding terminal stress state Q_j^a, the strain energy and complementary energy

$$W[q_j^a(\tau)] = \int_0^\tau Q_j\dot{q}_j \,\mathrm{d}t; \quad \Omega[Q_j^a(\tau)] = \int_0^\tau (Q_j^a - Q_j)\dot{q}_j \,\mathrm{d}t \tag{7}$$

are minimized and maximized, respectively, by the special paths expressed by Eqs. (6). (Only the homogeneity property Eqs. (5) is required; Ponter[1] derived this result for a somewhat more restricted class of viscous behavior).

With well defined functions of specific strain energy and specific complementary strain energy, the potential energy and complementary energy of a structure become well defined functions. Consider a structure subjected to specified loads (surface tractions) $p_i^s(x, \tau)$ on surface S_T and to constraints such that on surface S_u the displacements u_i are zero. (Here x denotes the coordinates of a generic point say on the center line of a beam or in the middle surface of a plate or shell; p_i^s, u_i^s, $i = 1,2,3$ are vector surface forces per unit area, and displacement, respectively; and the "surface" $S = S_T + S_u$ denotes the domain on which external forces or reactions are applied). Then the theorems of minimum potential energy and minimum complementary energy can be written (as if for a nonlinear elastic material), if extremal paths are followed. The potential energy theorem is

$$\int_V \check{W}[q_j^s(\tau)]\,\mathrm{d}V - \int_{S_T} p_i^s u_i^s \,\mathrm{d}S \leq \int_V \check{W}[q_j^c(\tau)]\,\mathrm{d}V - \int_{S_T} p_i^s u_i^c \,\mathrm{d}S \tag{8}$$

where integration over the "volume" V represents integration covering the whole structure; the system (u_i^c, q_j^c) satisfy the displacement boundary conditions and the equations of compatibility, i.e. conditions of kinematic admissibility; and the system (u_i^s, q_j^s) are not only kinematically admissible but (by extremal paths) lead to stresses Q_j^s which satisfy dynamic equations and stress boundary conditions, as well.

3. BOUNDS ON DYNAMIC DEFLECTIONS

Consider a structure subjected to impulsive loading on S_T so that there is an initial velocity $\dot{u}_i(x, 0) = \dot{u}_i^0(x)$, with initial displacements $u_i(x, 0) = 0$. The response velocities $\dot{u}_i(x, t)$ vanish at $t = t_f$, so that

$$\dot{u}_i(x, t_f) = 0, \quad u_i(x, t_f) = u_i^f(x). \tag{9}$$

We seek an upper bound on $u_i^f(x)$ for given $\dot{u}_i^0(x)$.

Consider the same structure subjected to statical loading (surface tractions) $p_i^s(x, t)$. The complete solution at time $t = \tau$, has strains $q_j^s(x, \tau)$ and stresses $Q_j^s(x, \tau)$ satisfying all kinematical and dynamical equations, where Q_j^s are related to q_j^s by the holonomic relations corresponding to extremal paths to the final strain state q_j^s. We may write the potential energy for the statically loaded structure at time τ as less than that computed for an alternative kinematically admissible displacement–strain system, in both cases the strain energy being computed for extremal paths. For the alternative system we take the system $u_i(x, \tau)$, $q_j(x, \tau)$ at time $t = \tau$ of the impulsively loaded structure. Equation (8) becomes

$$\int_V \check{W}[q_j^s(\tau)\,\mathrm{d}V - \int_{S_T} p_i^s(x, T)u_i^s(x, \tau)\,\mathrm{d}S \leq \int_V \check{W}[q_j(\tau)\,\mathrm{d}V - \int_{S_T} p_i^s(x, \tau)u_i(x, \tau)\,\mathrm{d}S. \quad (10)$$

The strain–time histories actually followed in the dynamic problem up to time τ are of course unknown. They are in general not extremal path histories for inelastic deformations, but in view of the definition Eq. (3) and conservation of energy for the impulsively loaded structure we can write

$$\int_V \check{W}[q_j(\tau)]\,\mathrm{d}V \leq \int_V W[q_j(\tau)]\,\mathrm{d}V = K_0 - K(\tau) \quad (11)$$

where

$$K_0 = \frac{1}{2}\int_V m\dot{u}_i^0\dot{u}_i^0\,\mathrm{d}V; \quad K(\tau) = \frac{1}{2}\int_V m\dot{u}_i(x, \tau)\dot{u}_i(x, \tau)\,\mathrm{d}V \quad (12)$$

are the kinetic energies at $t = 0$ and $t = \tau$ of the dynamically loaded structures; m is the specific mass in appropriate units. Combining Eqs. (10)–(12)

$$\int_V \check{W}[q_j^s(\tau)\,\mathrm{d}V - \int_{S_T} p_i^s(x, \tau)\, u_i^s(x, \tau)\,\mathrm{d}S \leq K_0 - K(\tau) - \int_{S_T} p_i^s(x, \tau)u_i(x, \tau)\,\mathrm{d}S. \quad (13)$$

Thus far, τ is arbitrary, but we may now set $\tau = t_f$, the time at which the impulsively loaded structure comes to rest and the final deformations $u_i^f(x)$ are reached. Using Eqs. (9) and rearranging, Eq. (13) becomes

$$\int_{S_T} p_i^s(u_i^f - u_i^{sf})\,\mathrm{d}S \leq K_0 - \int_V \check{W}[q_j^s(t_f)]\,\mathrm{d}V \quad (14)$$

where $u_i^{sf}(x)$ is the deflection at time t_f of the structure loaded statically by the surface tractions $p_i^s(x, t)$, with material behavior assumed that prescribed by extremal path histories to the final strain states. To obtain a bound on the displacement at $x = x_A$ in a direction corresponding to unit vector n_i, we take p_i^s as a concentrated force P_{An}^s in the given direction at x_A. If we choose $P_{An}^s(t)$ such that at $t = t_f$

$$\int_V \check{W}[q_j^s(t_f)]\,\mathrm{d}V = K_0 \quad (15a)$$

then by Eq. (14) we have

$$u_{An}^f \leq u_{An}^{sf}. \quad (15b)$$

Thus the bound on the final displacements of the impulsively loaded structure is provided by the solution of the static problem in which the static force applied at the point where the dynamic deflection is sought, and in its direction, produces a total strain energy equal to the given initial kinetic energy K_0 of the dynamic problem; the static problem is solved with the assumption that extremal paths are followed to the final states $u_i^{sf}(x)$, $q_j^{sf}(x)$, and are traversed in time t_f.

Equations (15) express the bounding theorem sought. It is valid for finite deflections and strains, and for very general inelastic material in which the time of traversal of strain or stress paths is a parameter affecting the resulting stress or strain, respectively.

We note that the theorem of Eqs. (15) requires knowledge of the time t_f at which the impulsively loaded structure comes to rest, Eq. (9). This time is of course unknown. It may however in certain cases be bounded above, and an upper bound on t_f enables an upper bound on the deflection to be computed. This will be illustrated. It turns out that the dependence on t_f is a weak one, so that rough estimates of t_f may suffice for many practical purposes, even when a rigorous upper bound is not available.

4. APPLICATIONS TO BEAM PROBLEMS

We illustrate the application of the bounding theorem stated above by showing the solutions of two problems of constrained beams. One is a simple discrete model with a single mass and a single "hinge" point, the other is a continuous beam of uniform mass and strength properties. In both cases the ends are fully fixed so as to prevent pull-in. For the discrete model an exact solution by numerical methods was obtained for comparison. For the fully constrained beam test results are available[14] as well as related analytical and approximate solutions. The main interest in these examples is in the large effects on the deformation magnitudes of the axial forces induced by the end constraints. These effects appear at finite deflections of the order of the beam thickness. For simplicity we shall use approximations appropriate to deflections that are small compared to the span. We shall also for simplicity assume inelastic behavior of viscous type, in which the constitutive equations relate stress to strain rate as in Eq. (5a). Strain hardening is not considered explicitly, but may be regarded as implicitly taken into account by the use of $\dot{q}_i(Q_k)$ relations for a chosen appropriate level of strain. This is reasonable for strongly rate sensitive metals of practical interest, for which the strain rate effect has been shown to predominate over strain hardening[15].

For constrained beam problems the constitutive equations needed are ones relating axial force N and bending moment M to center line extension rate $\dot{\epsilon}$ and and curvature rate $\dot{\kappa}$. When homogeneous relations are used the extremal path to a specified strain state (ϵ, κ) at a fixed time τ takes the simple form of Eq. (6). For convenience and simplicity we shall derive and use suitable homogeneous forms relating (N, M) and $(\dot{\epsilon}, \dot{\kappa})$.

These forms should express results of dynamic tests on beams with prescribed $(\dot{\epsilon}, \dot{\kappa})$ histories, but such tests appear not to have been made except for $\dot{\epsilon} \cong 0$, $N \cong 0$ (Rawlings[16], Aspden and Campbell[17]). We must therefore derive the needed constitutive forms by integration over the beam section, using stress–strain rate relations furnished by tests in simple tension and compression. We shall do this in the simplest way by assuming that the beam section is a sandwich beam with flange separation h and total area A. For rigid–perfectly plastic behavior the interaction between M and N is linear in each quadrant; for example

$$\frac{N}{N_0} + \frac{M}{M_0} = 1 \tag{16}$$

for $0 < N \leq N_0$; $0 \leq M \leq M_0$, with similar equations for the other quadrants, Fig. 2. Here N_0, M_0 are the plastic limit magnitudes in pure axial loading and pure bending, respectively. For a

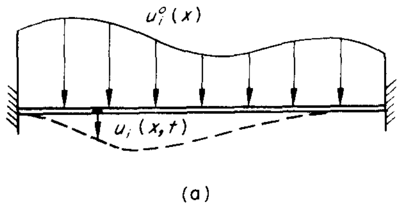

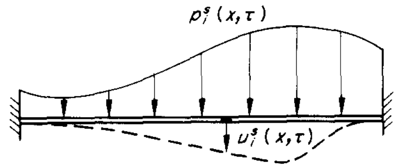

Fig. 1. (a) Typical problem of initial velocities due to impulsive loading. (b) Artificial static loading for deflection bound theorem.

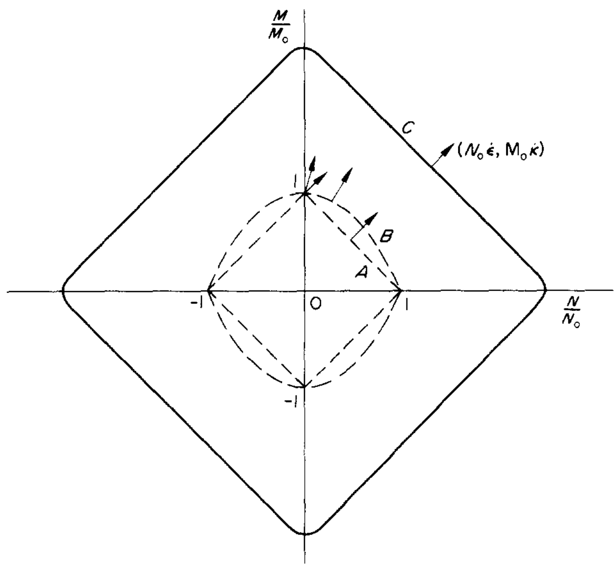

Fig. 2. Bending moment–axial force diagrams for beam. Curves A, B are yield diagrams for rigid–perfectly plastic material (curve A for sandwich beam, B for rectangular section). Curve C shows typical curve Ψ = constant for time dependent (homogeneous viscous) material.

rectangular section the corresponding relation is a parabolic curve, as indicated by the dashed curve in Fig. 2; hence the assumption of a sandwich beam involves an approximation on the conservative side, i.e. replaces the actual section by a weaker one. Hence it is appropriate here.

For dynamic straining of a rate dependent material we take $\dot{\epsilon}$ and $\dot{\kappa}$ to be given by differentiation of a homogeneous potential function of M and N. It is convenient to use dimensionless quantities (N/N_0'), (M/M_o'); $(\dot{\epsilon}/\dot{\epsilon}_0)$, $(\dot{\kappa}/\dot{\kappa}_0)$ where N_0', M_0', $\dot{\epsilon}_0$, $\dot{\kappa}_0$ are constants expressing material and section properties. These will be discussed shortly. We write

$$N_0'\dot{\epsilon} = \frac{\partial\Psi}{\partial(N/N_0')}, \quad M_0'\dot{\kappa} = \frac{\partial\Psi}{\partial(M/{}'_0)} \tag{17}$$

where

$$\Psi = \Psi\left(\frac{N}{N_0'}, \frac{M}{M_0'}\right).$$

A typical curve Ψ = constant is sketched in Fig. 2 showing some typical normal vectors ($N_0\dot{\epsilon}$, $M_0\dot{\kappa}$).

We showed in reference[18] that a homogeneous stress–strain rate relation may be substituted for a more realistic inhomogeneous one by choice of constants appropriate for a particular problem of impulsive loading. Suppose the "more realistic" form is

$$\frac{\sigma}{\sigma_0} = 1 + \left(\frac{\dot{\epsilon}}{\dot{\epsilon}_0}\right)^{1/n} \quad \text{for} \quad \dot{\epsilon} > 0; \quad -1 < \frac{\sigma}{\sigma_0} < 1 \quad \text{for} \quad \dot{\epsilon} = 0 \tag{18}$$

where σ_0, $\dot{\epsilon}_o$, and n are constants chosen to match simple tension/compression data of stress σ vs strain rate $\dot{\epsilon}$ in a certain range of strain rate and at a chosen strain level. (With three disposable constants the above form enables an excellent fit to be made with strain rate test data for rate sensitive metals such as mild steel or titanium. The typical concave upward shape when σ is plotted against log $\dot{\epsilon}$ is indicated in Fig. 3.) The above inhomogeneous form may be replaced by

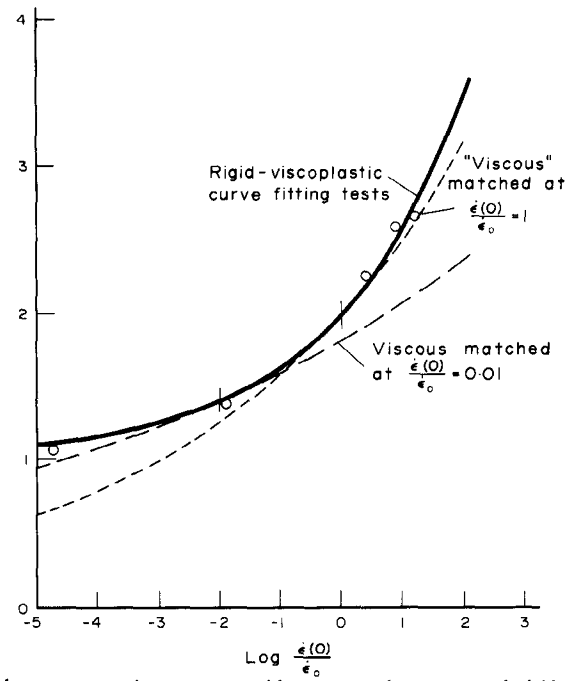

Fig. 3. Illustrations of homogeneous viscous curves with constants chosen to match rigid-viscoplastic curve and test points (mild steel, $n = 5$, $\dot{\epsilon}_0 = 40\ \text{sec}^{-1}$).

the following homogeneous one

$$\frac{\sigma}{\sigma_0'} = \left(\frac{\dot{\epsilon}}{\dot{\epsilon}_0}\right)^{1/n'}. \tag{19}$$

This form has two independent constants. We have chosen $\dot{\epsilon}_0$ in Eq. (19) the same as in Eq. (18), but have introduced new constants σ_0', n' related to those of Eq. (18) by

$$\sigma_0' = \mu\sigma_0, \quad n' = \nu n \tag{20}$$

If μ and ν are picked, as proposed in [18], so that the two curves of Eqs. (18) and (19) touch with a common tangent at a particular strain rate $\dot{\epsilon}(0)$, then the viscous curve Eq. (19) always lies below the curve of Eq. (18) see Fig. 3. Matching contact point and tangent at $\dot{\epsilon}(0)/\dot{\epsilon}_0 = \bar{v}_0$,

$$\nu = (1 + \bar{v}_o^{1/n})/\bar{v}_o^{1/n}; \quad \mu = (1 + \bar{v}_o^{1/n})/\bar{v}_0^{1/\nu n}. \tag{21}$$

Using these in Eqs. (20) for each initial strain rate $\dot{\epsilon}(0)$ in a one degree of freedom problem of impulsive loading, the viscous form Eq. (19) leads to final deformations essentially the same as those obtained by use of Eq. (18), the differences being less than 0·5 per cent, with $\bar{v}_0$ ranging from 10^{-4} to 10^3. Moreover since the replacement curve lies below the "more realistic" one, the approximation is conservative.

In problems where the initial velocity $\dot{u}_i^0(x)$ is given, the initial maximum strain rate is not specified in advance, but has to be estimated from the response. This means that an initial guess must be made for the initial relative strain rate $\bar{v}_0$, μ and $n' = \nu n$ calculated from Eqs. (21), and characteristics of the response determined. This furnishes a better value of $\bar{v}_0$, and the cycle must be repeated. This process converges rapidly, and one repetition of the cycle suffices, as will be illustrated. The simplifications of working with homogeneous forms seem well worth the additional effort, which is not large.

To obtain the desired homogeneous constitutive relations for the sandwich beam, we assume that each flange obeys the viscous law Eq. (19). It is straight-forward then to derive the relations for $N \geqslant 0$, $M \geqslant 0$:

$$\frac{\dot{\epsilon}}{\dot{\epsilon}_0} = \frac{1}{2}\left\{\left(\frac{N}{N_0'} + \frac{M}{M_0'}\right)^{n'} + \operatorname{sgn}\left(\frac{N}{N_0'} - \frac{M}{M_0'}\right)\left|\frac{N}{N_0'} - \frac{M}{M_0'}\right|^{n'}\right\} \tag{22a}$$

$$\frac{\dot{\kappa}}{\dot{\kappa}_0} = \frac{1}{2}\left\{\left(\frac{N}{N_0'} + \frac{M}{M_0'}\right)^{n'} + \operatorname{sgn}\left(\frac{M}{M_0'} - \frac{N}{N_0'}\right)\left|\frac{N}{N_0'} - \frac{M}{M_0'}\right|^{n'}\right\} \tag{22b}$$

where

$$M_0' = \mu M_0 = \frac{1}{2}\mu A h \sigma_0; \quad N_0' = \mu N_0 = \mu A \sigma_0$$

so that

$$\frac{M_0'}{N_0'} = \frac{M_0}{N_0} = \frac{\dot{\epsilon}_0}{\dot{\kappa}_0} = \frac{h}{2}. \tag{22c}$$

The above expressions correspond to Eq. (17) with

$$\Psi = \frac{N_0'\dot{\epsilon}_0}{2(n'+1)}\left\{\left(\frac{N}{N_0'}+\frac{M}{M_0'}\right)^{n'+1}+\left|\frac{N}{N_0'}-\frac{M}{M_0'}\right|^{n'+1}\right\}. \tag{23}$$

Similar forms for the remaining three quadrants are obvious by inspection.

(a) *Discrete mass example*

It is instructive to outline first the application of the bound theorem derived above to the structure model Fig. 4 consisting of a lump mass G connected by weightless members of length l to fixed supports. These members are rigid except for a discrete element at the midpoint where length changes e and bending rotations ψ occur. The rates of extension $\dot{e}$ and of rotation $\dot{\psi}$ are supposed related to the axial force N and bending moment M in the same way as $\dot{\epsilon}$ and $\dot{\kappa}$ according to Eqs. (22).

The mass G is subjected to an impulse so that its initial velocity is V_0. It finally comes to rest at time t_f with final displacement u_m^f. We seek an upper bound on u_m^f, supposing that the supports prevent pull-in but allow rotations of the rigid members. Such a bound is furnished by the displacement u_m^{sf} of the same structure model loaded statically by a force p_m^{sf} applied in such a way that at time t_f the total work done, computed on the assumption that extremal paths are followed, is equal to the initial kinetic energy $K_0 = \frac{1}{2}GV_0^2$ of the dynamically loaded structure. In other words, $u_m^f \leq u_m^{sf}$ provided $K_0 = \int_V \check{W}[\psi^{sf}(t_f)]\,dV$, where ψ^{sf} is the rotation associated with μ_m^{sf}, and $\check{W}$ is the minimum work for the strain state ψ^{sf} reached at time t_f. In view of Eqs. (5) we have

$$\check{W}[\psi^{sf}(t_f)] = \text{ep}\int_0^{t_f} Q_i\dot{q}_i\,dt = \text{ep}\int_0^{t_f} Q_i\frac{\partial\Psi}{\partial Q_i}\,dt = \text{ep}\int_0^{t_f}(n+1)\Psi\,dt. \tag{24}$$

For the sandwich beam we write

$$\Psi = \frac{N_0'\dot{e}_o}{2(n'+1)}\left\{\left(\frac{N^s}{N_0'}+\frac{M^s}{M_0'}\right)^{n'+1}+\left|\frac{N^s}{N_0'}-\frac{M^s}{M_0'}\right|^{n'+1}\right\} \tag{25}$$

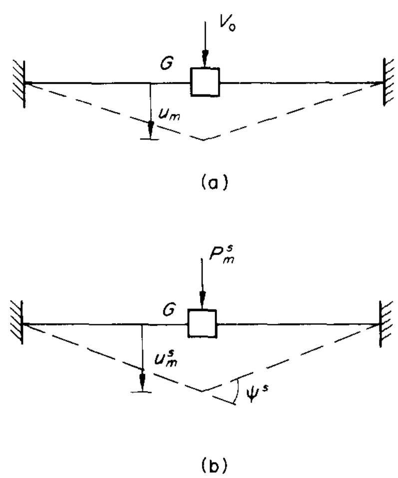

Fig. 4. One degree of freedom structure model. (a) Impulsive loading. (b) Artificial static loading.

where $\dot{e}_0$ is a material constant with dimensions of length/time, corresponding to the constant of strain rate sensitivity $\dot{\epsilon}_0$ in Eq. (18). Minimum work is achieved by the extremal paths

$$0 \leqslant t < t_f: \quad M^s(t) = \frac{n'}{n'+1} M^{sf}, \quad N^s(t) = \frac{n'}{n'+1} N^{sf}; \quad M^s(t_f) = M^{sf}, N^s(t_f) = N^{sf}. \tag{26}$$

Using these in Eqs. (24) and (25), the energy condition takes the form

$$K_0 = \frac{1}{2} N_0' \dot{e}_0 t_f \left(\frac{n'}{n'+1}\right)^{n'+1} [(s+m)^{n'+1} + |s-m|^{n'+1}] \tag{27}$$

with

$$s = \frac{N^{sf}}{N_0'}, \quad m = \frac{M^{sf}}{M_0'}. \tag{28}$$

The corresponding displacement u_m^{sf} is obtained by integrating the rotation rate over time t_f; if $(N/N_0') \geqslant (M/M_0')$,

$$\dot{u}_m^s(t) = \frac{l}{2} \dot{\psi}^s(t) = \frac{l\dot{e}_0}{2h} \left[\left(\frac{N}{N_0'} + \frac{M}{M_0'}\right)^{n'} - \left(\frac{N}{N_0'} - \frac{M}{M_0'}\right)^{n'} \right] \tag{29}$$

$$u_m^{sf} = \frac{l}{2} \int_0^{t_f} \dot{\psi}^s \, \mathrm{d}t = \frac{l\dot{e}_0 t_f}{2h} \left(\frac{n'}{n'+1}\right)^{n'} [(s+m)^{n'} - (s-m)^{n'}]. \tag{30}$$

The condition of end fixity requires the extension at the hinge element to equal the increase of length of the centerline due to the deflection. With deflections small compared to the span the change of centerline length is given closely by

$$\Delta L = \frac{1}{2} \int_0^L \left(\frac{\partial u}{\partial x}\right)^2 dx \tag{31}$$

where L is the span. Applying this to the simple model the constraint–extension condition furnishes the equation (if $N/N_0' > M/M_0'$)

$$\frac{1}{l}(u_m^{sf})^2 = \int_0^{t_f} \dot{e} \, \mathrm{d}t = \frac{1}{2} \dot{e}_0 t_f \left(\frac{n'}{n'+1}\right)^{n'} [(s+m)^{n'} + (s-m)^{n'}]. \tag{32}$$

Now Eqs. (30) and (32) may be solved for $s + m$ and $s - m$, which may then be substituted in Eq. (27) to obtain a relation between the input energy K_0 and the bounding displacement u_m^{sf}

$$K_0 = \frac{1}{2} M_0' \left(\frac{2\dot{e}_0 t_f}{h}\right)^{-(1/n')} \left(\frac{2h}{l} \delta_m\right)^{1+(1/n')} [(\delta_m + 1)^{1+(1/n')} + (\delta_m - 1)^{1+(1/n')}] \tag{33}$$

where

$$\delta_m = \frac{u_m^{sf}}{h}. \tag{34}$$

It is convenient to introduce further dimensionless variables

$$\lambda = \frac{4K_0}{P_m{}^L h} = \frac{GlV_0{}^2}{M_0 h}; \quad \eta = \frac{t_f}{t_f^c} = \frac{2M_0}{GlV_0} t_f. \tag{35}$$

Together with the previously defined

$$\mu = \frac{M_0'}{M_0}, \nu = \frac{n'}{n}, \quad \text{and} \quad \bar{v}_0 = \frac{\dot{\epsilon}(0)}{\dot{\epsilon}_0}.$$

Eq. (33) takes the form

$$\lambda^{1+(1/\nu n)} = 2\mu\left(\frac{2\bar{v}_0}{\eta}\right)^{(1/\nu n)} \delta_m{}^{1+(1/\nu n)}[(\delta_m + 1)^{1+(1/\nu n)} + (\delta_m - 1)^{1+(1/\nu n)}]. \tag{36}$$

This equation provides the upper bound sought. For a given value of λ the corresponding value of δ_m obtained from Eq. (36) bounds $u_m{}^f/h$, $u_m{}^f$ being the final displacement of the impulsively loaded structure,

$$\frac{u_m{}^f}{h} \leq \delta_m. \tag{37}$$

This result Eq. (36) requires numerical values of $\bar{v}_0$ and η. Of these, $\bar{v}_0$ is the initial strain rate in the structure divided by the quantity $\dot{\epsilon}_0$ which is a material constant which is very large for a weakly rate sensitive material and relatively small for one with strong rate sensitivity (e.g. of the order of 50 sec^{-1} for mild steel). In the present example $\bar{v}_0 = 2V_0/l\dot{\psi}_0$, $2V_0/l$ being the initial hinge rotation rate due to the impulsive loading and $\dot{\psi}_0 = 2\dot{e}_0/h$. The present example is intended to show basic ideas of the method, so for simplicity we put

$$\bar{v}_0 = C\sqrt{\lambda}, \quad C = \frac{h}{l\dot{e}_0}\sqrt{\frac{M_0 h}{Gl}}. \tag{38}$$

For example if we take $C = 0{\cdot}1$, then $\bar{v}_0 = 1$ at $\lambda = 100$; this enables us at least to compare results for different material constants or structural dimensions. In the second example we discuss a more practical problem of evaluation of $\bar{v}_0$. Recall that $\bar{v}_0$ is needed in order to determine the appropriate values of the factors μ and ν used in the process of matching a homogeneous viscous form to the rigid–viscoplastic one, by Eqs. (21). With Eq. (38), Eq. (36) becomes

$$\lambda^{1+(1/2\nu n)} = 2\mu\left(\frac{2C}{\eta}\right)^{(1/\nu n)} \delta_m{}^{1+(1/\nu n)}[(\delta_m + 1)^{1+(1/\nu n)} + (\delta_m - 1)^{1+(1/\nu n)}]. \tag{39}$$

Finally, η must be chosen. This is defined in Eq. (35) as the ratio of the "stopping time" t_f of the dynamically loaded structure to t_f^c which is the lower bound according to Martin's theorem [2] for the deformation time of an impulsively loaded structure of rigid–perfectly plastic material. In the present problem t_f^c is not merely a lower bound but is the actual stopping time of the rigid–perfectly plastic structure. Hence it clearly provides an upper bound for the stopping time of the structure with rate dependent plastic behavior. Thus we may take $\eta = 1$ to obtain a sure upper bound on the final deflection of the present structure model. However the definition of η used above refers to the time bound t_f^c according to a small deflection theory. In Section 5 we discuss a time bound for the rigid–perfectly plastic structure which takes account of the strengthening effect due to full end fixity. The result is obtained that $\bar{t}_f^c = t_f^c/2\delta_m$. In Fig. 5 we have plotted the bound δ_m as function of λ, taking $\eta = 1$ and $\eta = 1/2\delta_m$; for both we have used $C = 0{\cdot}1$. In this figure are shown for comparison the "exact" final displacement computed by numerical integration. We show also a curve giving the bounds for large deflections of the rigid perfectly plastic structure model, i.e. for a non-rate sensitive material. These bounds are obtained by applying Martin and Ponter's method [6] for finite deflection bounds for a time independent plastic behavior. The resulting bound on $u_m^{\prime f}/h = \delta_m'$ is found to be

$$\delta_m' = \frac{1}{2}\sqrt{\lambda}. \tag{40}$$

This is valid for $\lambda \geq 4$. Finally, in Fig. 5 is drawn the straight line which gives the response if both end fixity and time dependence are neglected.

(b) *Fully constrained beam*

As a second example we consider a continuous beam with ends fixed so that rotations and pull-in are prevented. The beam has a span $4l$, constant mass per unit length m, and uniform plastic and viscoplastic properties. It is subjected to impulsive loading so that it has uniform initial velocity V_0. An analytical solution for rigid–perfectly plastic material behavior was given by Symonds and Mentel [19]. Martin and Ponter [6] obtained finite deflection bounds for this material. Tests on mild steel specimens were reported by Symonds and Jones [14], including results of numerical solutions for several cases. Data for these tests will be used to illustrate the application of the present approach to bounds for time dependent material. We shall assume viscous behavior of homogeneous form as expressed by Eq. (22), with factors μ and ν calculated by Eqs. (21) so as to match rigid–viscoplastic behavior at the initial maximum strain rate divided by the material rate

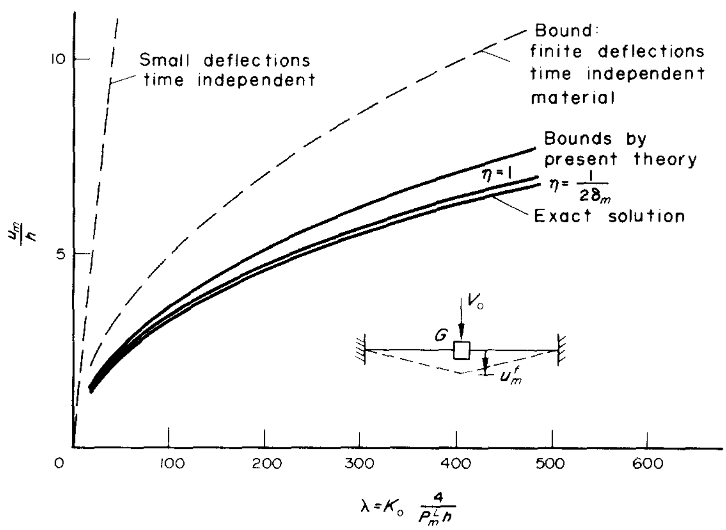

Fig. 5. Deflection bounds for one degree of freedom model. "Exact solution" obtained by numerical integration.

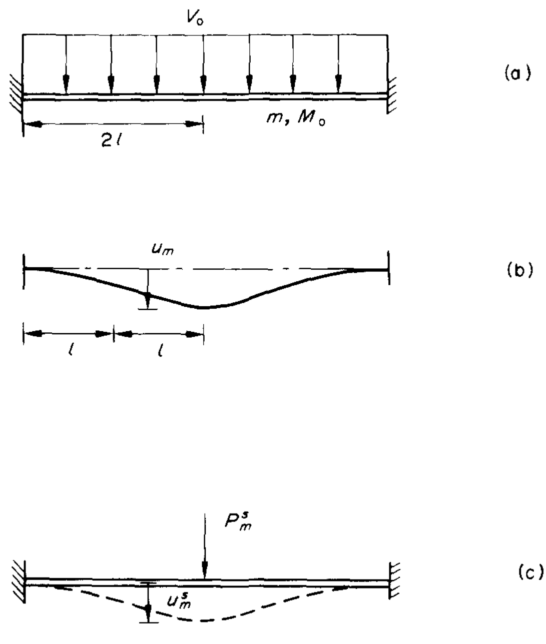

Fig. 6. Fully constrained beam example. (a) and (b) Show impulsive loading, final deflections. (c) Shows artificial static loading and corresponding deflection curve.

constant $\dot\epsilon_0$ and denoted by $\bar v_0$. The initial strain rates are unknown. They must be estimated from the initial velocity and knowledge about the strain distribution deduced from the theory. A way of doing this will be described. It will be seen that the results are insensitive to the ratio $\bar v_0$.

The application of the present bounds theory in this problem is basically similar to that outlined above for the discrete model. A bound on the final mid-point displacement u_m^f, reached at time t_f, is given by the displacement u_m^{sf} at the same point caused by a force P_m^s applied statically during the time interval t_f in such a way that the total work done is K_0, when the beam deformation occurs according to extremal paths so that that the total work is minimized for fixed final strain states. By symmetry we need consider only a quarter span. The energy condition can be written, following the procedure leading to Eq. (27), as

$$K_0 = 4\int_0^l \check{W}[u_m^{sf}(t_f)]\,\mathrm{d}x = 4\int_0^l \left\{\mathrm{ep}\int_0^{t_f}(n+1)\Psi\,\mathrm{d}t\right\}\mathrm{d}x$$
$$= 4N_0'\dot\epsilon_0 t_f\left(\frac{n'}{n'+1}\right)^{n'+1}\int_0^l [(s+m)^{n'+1}+|s-m|^{n'+1}]\,\mathrm{d}x \quad (41)$$

where

$$s = \frac{N^{sf}(x)}{N_0'},\; m = \frac{M^{sf}(x)}{M_0'} \quad (42)$$

are the final values of stress reached by the paths of Eqs. (26) which minimize the strain energy.

Determination of the bound now requires finding the functions $s(x)$ and $m(x)$ of the statical problem, so as to satisfy equilibrium conditions and the constraint–extension condition. We do this by an iterative process. Consider the free body diagrams of the quarter span, Fig. 7. We shall

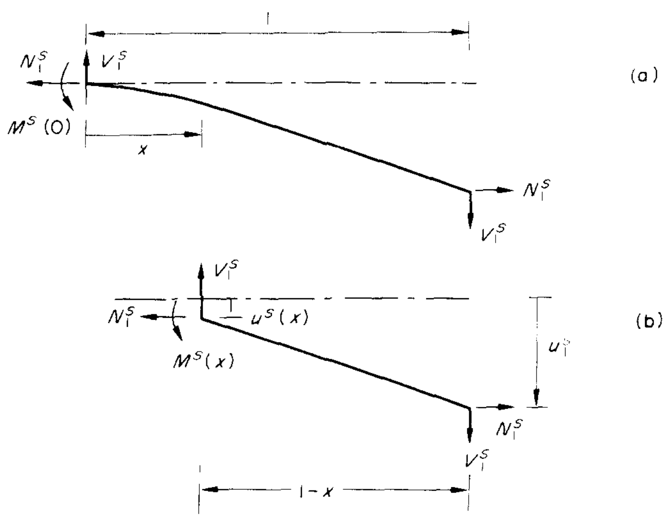

Fig. 7. Free body diagrams for statically loaded beam. (a) Quarter span of beam. (b) Part of quarter span.

assume that the deflections are small enough so that the axial force in the beam can be taken as

$$N^{sf}(x) = N_1^{sf} = \text{Constant} \tag{43}$$

and

$$M^{sf}(x) = V_1^{sf}(l-x) - N_1^{sf}(u_1^{sf} - u^{sf}(x)) \tag{44}$$

where N_1^{sf}, V_1^{sf} are horizontal and vertical forces at the quarter point of the beam $x = l$ (where $M^{sf}(l) = 0$ by symmetry), and $u_1^{sf} = u^{sf}(l)$ is the displacement at the quarter point. The deflection curve is almost linear, the deformations being largely concentrated at "hinge" zones near $x = 0$ and $x = 2l$. We may write the deflection curve as

$$u^{sf}(x) = u_1^{sf}\left[\frac{x}{l} + f\left(\frac{x}{l}\right)\right] \tag{45}$$

where $f(x/l)$ vanishes at $x = 0$ and $x = l$. Then we can write

$$s + m = s_1\left[1 + Z\left(1 - \frac{x}{l}\right) - \frac{N_0'}{M_0'} u_1^{sf} f\left(\frac{x}{l}\right)\right] \tag{46a}$$

$$s - m = s_1\left[1 - Z\left(1 - \frac{x}{l}\right) + \frac{N_0'}{M_0'} u_1^{sf} f\left(\frac{x}{l}\right)\right] \tag{46b}$$

where

$$s_1 = N_1^{sf}/N_0', Z = (V_1^{sf} l - N_1^{sf} u_1^{sf}) N_0'/M_0' N_1^{sf}. \tag{47}$$

Note that the curvature and axial strain are (for $s \geq m$)

$$\kappa^{sf} = u_{xx}^{sf} = \int_0^{t_f} \dot{\kappa}\,\mathrm{d}t = \frac{\dot{\epsilon}_0 t_f}{h}\left(\frac{n'}{n'+1}\right)^{n'}[(s+m)^{n'} - (s-m)^{n'}] \tag{48a}$$

$$\epsilon^{sf} = \int_0^{t_f} \dot{\epsilon}\,\mathrm{d}t = \frac{1}{2}\dot{\epsilon}_0 t_f\left(\frac{n'}{n'+1}\right)^{n'}[(s+m)^{n'} + (s-m)^{n'}]. \tag{48b}$$

We may start an iteration by dropping the term $u_1^{sf}f(x/l)N_0'/M_0'$ in Eqs. (46), so that $s+m$ and $s-m$ have linear variation with x. Equations (48) give the curvature and strain in terms of Z, s_1 and a numerical function of x. Thus s_1 can be found by applying the constraint–extension condition in terms of Z:

$$\frac{1}{2}\int_0^l (u_x^{sf})^2\,\mathrm{d}x = \int_0^l \mathrm{e}^{sf}\,\mathrm{d}x.$$

The slope $u_x^{sf}(x)$ is found from u_{xx}^{sf} by integration, putting

$$u_{xx}^{sf} \cong \frac{\dot{\epsilon}_0 t_f}{h}\left(\frac{n'}{n'+1}\right)^{n'} s_1^{n'}\left[\left(1+Z-Z\frac{x}{l}\right)^{n'} - \left(1-Z+Z\frac{x}{l}\right)^{n'}\right]. \tag{49}$$

Thus

$$\frac{1}{2}\int_0^l (u_x^{sf})^2\,\mathrm{d}x = \frac{1}{2}\left(\frac{\dot{\epsilon}_0 t_f}{h}\right)^2\left(\frac{n'}{n'+1}\right)^{2n'} s_1^{2n'} l^3 F(Z) \tag{50a}$$

and

$$\int_0^l \mathrm{e}^{sf}\,\mathrm{d}x = \frac{1}{2}\dot{\epsilon}_0 t_f\left(\frac{n'}{n'+1}\right)^{n'} s_1^{n'} l G(Z) \tag{50b}$$

where

$$F(Z) = \int_0^1 \left\{\int_0^\xi [(1+Z-Z\alpha)^{n'} - (1-Z+Z\alpha)^{n'}]\,\mathrm{d}\alpha\right\}^2 \mathrm{d}\xi \tag{51a}$$

$$G(Z) = \int_0^1 [(1+Z-Z\xi)^{n'} + (1-Z+Z\xi)^{n'}]\,\mathrm{d}\xi. \tag{51b}$$

The constraint–extension condition thus furnishes

$$\frac{n'}{n'+1}s_1 = \left[\frac{h^2}{l^2\dot{\epsilon}_0 t_f}\frac{G(Z)}{F(Z)}\right]^{1/n'}. \tag{52}$$

We have also, by direct integration from Eq. (49)

$$\frac{u_m^{sf}}{h} = \frac{2u_1^{sf}}{h} = \frac{2l^2\dot{\epsilon}_0 t_f}{h^2}\left(\frac{n'}{n'+1}\right)^{n'} s_1^{n'} H(Z) \tag{53a}$$

and

$$K_0 = 8lM_0'\frac{\dot{\epsilon}_0 t_f}{h}\left(\frac{n'}{n'+1}\right)^{n'+1} s_1^{n'+1} I(Z) \tag{53b}$$

where

$$H(Z) = \int_0^1 (1-\xi)[(1+Z-Z\xi)^{n'} - (1-Z+Z\xi)^{n'}]\,d\xi$$

$$I(Z) = \int_0^1 [(1+Z-Z\xi)^{n'+1} + (1-Z+Z\xi)^{n'+1}]\,d\xi. \tag{54b}$$

If we now use the result Eq. (52) for s_1, in Eqs. (53), and use the dimensionless variables

$$\lambda = \frac{4K_0}{P_m{}^L h} = \frac{4ml^2}{M_0}\frac{V_0{}^2}{h}; \quad \delta_m = \frac{u_m{}^{sf}}{h} \tag{55}$$

we obtain

$$\lambda = 16\mu\left(\frac{h^2}{l^2\dot{\epsilon}_0 t_f}\right)^{1/n'} I(Z)\left[\frac{G(Z)}{F(Z)}\right]^{1+(1/n')} \tag{56}$$

$$\delta_m = \frac{2G(Z)H(Z)}{F(Z)}. \tag{57}$$

It is seen that, apart from the factor $(h^2/l^2\dot{\epsilon}_0 t_f)^{1/n'}$, a numerical choice of Z in Eqs. (56) and (57) leads to the bound δ_m for the corresponding energy parameter λ. Our equations are written for $s \geq m$, so that we take values $0 \leq Z \leq 1$. (Physically by Eq. (44) the parameter Z as defined in Eq. (47) represents the ratio of the net moment at $x = 0$ to the axial force $N_1{}^{sf}$ times $h/2$; thus small Z corresponds to large deflections, with "membrane effects" predominating over bending.)

Thus we have the desired bound

$$\frac{u_m{}^f}{h} \leq \delta_m(\lambda) \tag{58}$$

by inserting values of $Z \leq 1$ in Eqs. (56) and (57), *provided* we can assign realistic values to the factor $(h^2/l^2\dot{\epsilon}_0 t_f)^{1/n'}$. This factor involves the unknown time t_f at which deformation ceases in the dynamic problem. In addition, we must be able to estimate the "initial relative strain rate" $\bar{v}_0 = \dot{\epsilon}(0)/\dot{\epsilon}_0$, in order to obtain the constants μ and ν by Eq. (21) which enable us to match the homogeneous viscous form Eq. (19) to the rigid–viscoplastic one of Eq. (18). Fortunately the results are insensitive to the choices both of t_f and of $\bar{v}_0$.

To deal with the first difficulty, that of estimating t_f, we again introduce the ratio η of t_f to the lower bound $t_f{}^c$ computed by Martin's theorem for a rigid–perfectly plastic structure with small deflections. In the present example we have

$$t_f = \eta t_f{}^c = \eta\frac{ml^2V_0}{M_0}. \tag{59}$$

We write V_0 in terms of λ and constants of the structure from the definition Eq. (55). Thus we obtain

$$\frac{h^2}{l^2\dot{\epsilon}_0 t_f} = \frac{1}{\eta\sqrt{\lambda}}\frac{2h^2}{\dot{\epsilon}_0 l^3}\sqrt{\frac{M_0}{hm}} = \frac{1}{\eta\sqrt{\lambda}}\frac{\sqrt{2}h^2}{\dot{\epsilon}_0 l^3}\sqrt{\frac{\sigma_0}{\rho}} \tag{60}$$

having made use of $M_0 = \sigma_0 Ah/2$, $m = A\rho$, where σ_0 is the static yield stress and ρ is the mass per unit volume. Thus $h^2/l^2\dot{\epsilon}_0 t_f$ can be evaluated numerically for a particular structure and material in terms of η and λ. Now $\eta = 1$ certainly provides an *upper* bound on t_f for the rate dependent material; t_f^c here clearly gives the actual deformation time for the small deflection–rate independent problem, and t_f is less than t_f^c because the strain rate sensitivity raises stress levels and shortens the stopping time. Thus if we put $\eta = 1$ we will obtain a valid upper bound on the deflection of the viscoplastic case. We can do better, however, by modifying Martin's small deflection time bound theory to take account of finite deflections when the ends are fully constrained. This is discussed in the next Section, where it is shown that for the fixed-ended beam it is appropriate to take

$$\eta \leqslant \frac{1}{u_m^f/h} = \frac{1}{\delta_m} \tag{61}$$

the two values $\eta = 1$ and $\eta \times 1/\delta_m$ are used in the illustrative example, taking constants for one of the series of mild steel beams tested by Symonds and Jones[14], namely $h = 0{\cdot}1$ in., $l = 1{\cdot}25$ in., $\dot{\epsilon}_0 = 40\ \mathrm{sec}^{-1}$, $\sigma_0 = 30\times 10^3$ psi, $n = 5$, $\rho = 0{\cdot}73\times 10^{-3}$ lb. sec^2/in^4. Putting these in Eq. (56) we obtain finally

$$\lambda^{1+(1/2\nu n)} = 16\mu\left(\frac{\sqrt{2}h^2}{\eta\dot{\epsilon}_0 l^2}\sqrt{\frac{\sigma_0}{\rho}}\right)^{1/\nu n} I(Z)\left[\frac{G(Z)}{F(Z)}\right]^{1+(1/\nu n)} \tag{62}$$

where, with the numbers listed above

$$\frac{\sqrt{2}h^2}{\dot{\epsilon}_0 l^3}\sqrt{\frac{\sigma_0}{\rho}} = 1{\cdot}16. \tag{63}$$

Finally a means of estimating the initial maximum strain rate must be provided. The initial uniform velocity distribution must be used together with information about the deflection shape gained from the present theory. We do this by adopting the point of view of the mode approximation technique[20]. Thus we write the velocity pattern of the beam in mode form, i.e. with separated variables

$$\dot{u}^* = \alpha T(t)\phi(x) \tag{64}$$

where $T(t)$ is a function such that $T(0) = 1$, $\phi(x)$ is the constant "shape function" (also normalized in any convenient way), and α is a scalar factor which may be chosen to give a "best fit" with the given initial velocity distribution for a chosen function $\phi(x)$. For initial uniform velocity V_0 and $\phi(x) = x/2l$, the method of [20] gives $\alpha = 3/2\,V_0$. Now we may write the initial curvature rate as

$$\dot{u}^{*0}_{xx}(x) \cong \frac{3}{2}V_0\frac{u^{sf}_{xx}(x)}{u_m^{sf}} \tag{65}$$

where u^{sf}_{xx} is the curvature function generated by the static solution for the force P_m^{sf}. In other words, we are computing the amplitude factor $3/2V_0$ from the approximate linear deflection curve, but we are using the curvature distribution generated by the non-linear viscous behavior corresponding to equilibrium requirements of the statically loaded and fully constrained beam. The maximum initial strain rate is $(h/2)\dot{u}^{*}_{xx}(0)$; hence $\bar{v}_0$ is given by

$$\bar{v}_0 \cong \frac{\dot{\epsilon}(0)}{\dot{\epsilon}_0} = \frac{h}{2\dot{\epsilon}_0}\frac{3}{2}V_0\frac{u_{xx}^{sf}(0)}{u_m^{sf}} = \sqrt{\lambda}\frac{3}{16}\frac{h}{\dot{\epsilon}_0 l^3}\sqrt{\frac{M_0 h}{m}}J(Z) \tag{66}$$

where

$$J(Z) = \frac{(1+Z)^{n'} - (1-Z)^{n'}}{H(Z)}. \tag{67}$$

For the beam test data as given above, we obtain

$$\bar{v}_0 = 0{\cdot}109\, J(Z)\sqrt{\lambda} \tag{68}$$

In Fig. 8 are plotted the upper bound curve $\delta_m(\lambda)$ using Eqs. (57) and (62) together with Eqs. (68) and (21); η has been assigned the two values $\eta = 1$ and $\eta = 1/\delta_m$. An iterative procedure is necessary, starting with a chosen value of Z and a "guessed" value of $\bar{v}_0$. This is illustrated by the calculations for $Z = 0{\cdot}5$ shown below. Rapid convergence due to weak dependence of μ and ν on $\bar{v}_0$ is evident. (The method "works" efficiently because of this, in fact). The bounding curve lies above the test points and the exact values obtained by finite difference numerical integration quoted from[14]. It lies below the bounding curve[6] and the solution curve[19] for rate independent behavior. The linear solution when constraint and rate effects are both neglected is also shown; it is wildly inaccurate except for $u_m/h \ll 1$.

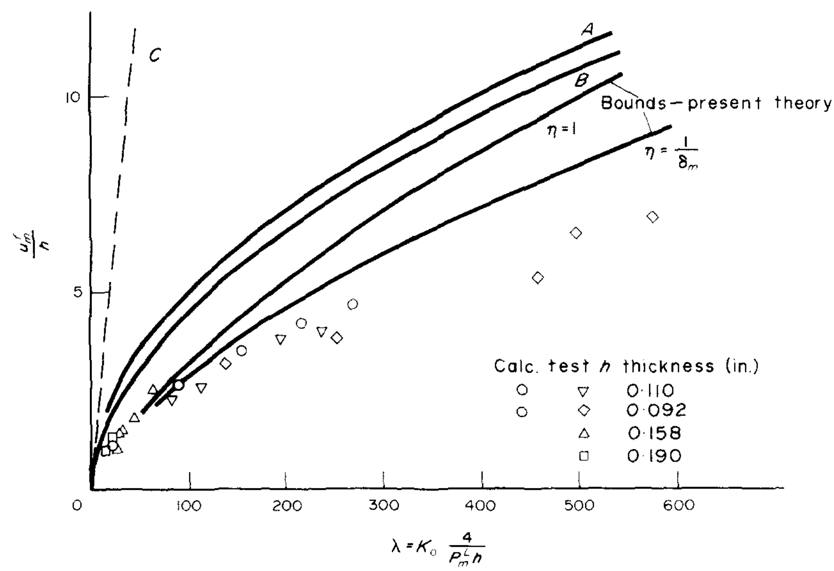

Fig. 8. Fully constrained beam with uniform impulsive loading, comparison of deflection bounds from present theory with test results and numerically computed values from Ref. [14]. Comparisons also shown: Curve A deflection bound for rigid–perfectly plastic material [6]; Curve B solution for rigid–perfectly plastic case [19]; Curve C solution for rigid–perfectly plastic case for small deflections [19].

Cycle	$\bar{v}_o$	μ	$n' = 5\nu$	δ_m	λ
1	1	2	10	4·76	153·3
2	6·58	1·965	8·43	5·01	189·0
3	6·40	1·966	8·45	5·01	189·1

5. TIME BOUND FOR FINITE DEFLECTIONS

In the following we propose a modification of Martin's[2] approach to a lower bound on deformation time, to take account of finite deflections. It applies to a structure of rigid–perfectly plastic (rate independent) material. We know (Nayfeh and Prager [2]) that in many circumstances Martin's time bound provides an exact result for a structure of that material. (It is almost always a good approximation, even when not exact). In these circumstances it provides an *upper* bound for the same structure of rate dependent rather than rigid–perfectly plastic material, since the deflection shapes do not differ greatly in the two cases.

Martin's time bound theorem is based on the convexity–normality inequality for time independent plastic flow

$$(Q_i - Q_i^a)\dot{q}_i \geq 0 \tag{69}$$

(where Q_i is the stress at which plastic strain rates $\dot{q}_i$ occur, and Q_i^a satisfies the yield condition $\phi(Q_i^a) \leq 0$), and makes use of the principle of virtual work rate for small deflections. A time independent velocity field $\dot{u}_i^c = \phi_c^c(x)$ and associated strain rate field $\dot{q}_j^c = k_j^c(x)$ are introduced, these satisfying kinematic requirements (compatibility and zero velocity boundary conditions); stresses $Q_j^c(x)$ correspond to $k_j^c(x)$ through Eq. (69). Consider now a structure with initial deflections, in particular whose initial center-line curve or middle surface differs from the actual initial curve or surface by the final displacements $u_i^f(x) = u_i(x, t_f)$ of the structure due to impulsive loading such that its initial velocities were $\dot{u}_i^0(x) = u_i(x, 0)$. Applying the technique of Martin's theorem to the structure with initial deflections, we obtain

$$t_f \geq \bar{t}_f^c = \frac{\int_V m\dot{u}_i^0\phi_i^c \, \mathrm{d}V}{\int \bar{Q}_j^c k_j^c \, \mathrm{d}V} \tag{70}$$

where we have written the specific energy dissipation rate as $\bar{Q}_j^c k_j^c$ to emphasize that this quantity is to be computed for the fictitious structure with initial deflections rather than the actual structure. Otherwise the argument is the same as for Martin's result of identical form.

Applying this to the discrete structure model of example (a), we choose velocity field $\dot{u}_m^c = \phi_m^c = 1$, with rotation rate $\dot{\psi}^c = 2/l$ across the hinge. The dissipation rate corresponding to the linear yield curve of Eq. (16) is

$$\bar{Q}_i^c k_i^c = N\dot{e} + M\dot{\psi} = \frac{N}{N_0}(N_0\dot{e}) + \frac{M}{M_0}(M_0\dot{\psi}). \tag{71}$$

We must take account of the flow rule, which requires the strain rate vector $(N_0\dot{e}, M_0\dot{\psi})$ to be normal to the straight sides of the yield curve (hence $N_0\dot{e} = M_0\dot{\psi}$ in the first quadrant) or within the the angle defined by adjacent normals at its corners. There are three possibilities for $0 \leq N \leq N_0$, $0 \leq M \leq M_0$:

(a) $N = 0$: $M = M_0, \bar{Q}_j^c k_j^c = M_0 \dot{\psi}^c$ (72a)

(b) $0 < \frac{N}{N_0} < 1, 0 < \frac{M}{M_0} < 1$: $\bar{Q}_j^c k_j^c = M_0 \dot{\psi}^c = N_o \dot{e}^c$ (72b)

(c) $M = 0$: $N = N_0, \bar{Q}_j^c k_j^c = N_0 \dot{e}^c$. (72c)

For the fixed end condition, since the structure model has initial midpoint displacement u_m^f, the total extension rate $\dot{e}^c = 2u_m/l$. Thus except for case (a) with $N = 0$, $\bar{Q}_j^c k_j^c = 2N_0 u_m/l$. Putting this in Eq. (70), we obtain

$$\bar{t}_f^c = \frac{GV_0 l}{2N_0 u_m} = \frac{t_f^c}{N_0 u_m/M_0} = \frac{t_f^c}{2\delta_m} \tag{73}$$

where $\delta_m = u_m/h$, and $t_f^c = GV_0 l/2M_0$ is the time lower bound for case (a) (the usual small deflection result of Martin's theorem). The time bound for finite deflections of Eq. (73) corresponds to the choice $\eta = 1/2\delta_m$, which leads to the more realistic deflection bound for the discrete model, as indicated by the curve in Fig. 5.

For the continuous beam problem example (b), we choose velocity field $\dot{u}^c = \phi^c(x) = x/2l$. We obtain for $N \neq 0$

$$\int_V \bar{Q}_j^c k_j^c \, \mathrm{d}V = 4\int_0^l N_0 \dot{\epsilon}^c \, \mathrm{d}x = N_0(u_m^f/l) \tag{74}$$

$$\bar{t}_f^c = \frac{2mlV_0}{N_0 u_m^f/l} = \frac{2M_0 t_f^c}{N_0 u_m^f} = \frac{t_f^c}{\delta_m} \tag{75}$$

where t_f^c is the small deflection bound, Eq. (59). This result corresponds to the choice $\eta = 1/\delta_m$ used in the calculated bounding curve for example (b), shown in Fig. 8.

6. DISCUSSION AND CONCLUSIONS

The computed upper bounds lie above the deflection magnitudes obtained by numerical integration in the example of a simple discrete model, and those observed in tests in the example of a beam with full end fixity. In the latter case the bounds are appreciably higher than the deflection magnitudes obtained in tests and by numerical finite difference calculations (Fig. 8), while for the discrete model they are quite close to the "exact" solution obtained numerically. This difference may be due to the use of a sandwich beam model for the computed bound instead of a rectangular section used in the tests and simulated by the finite-difference model. This and other simplifying approximations all are conservative, i.e. tend to raise the computed bound.

The need to estimate or bound from above the actual deformation time is a defect of the present approach. (The same difficulty appears also in Martin's small deflection bound theory[7]). Although the upper bounds obtained here from the rigid plastic bound are valid for the examples discussed and for other cases where the main deforming zones of the dynamically deforming structure can be identified intuitively, it would be advantageous to have a rigorous theory for upper bounds on time of deformation.

The present method requires the solution of a problem of static loading of a time dependent material for finite deflections, and this requires considerably more effort than do the bounds theorems previously given for small displacements, even with the simplifications of deflection geometry and homogeneous viscous behavior adopted here. A more systematic approach, undoubtedly by numerical methods, will be necessary in order to deal with more complex structures, arbitrarily large deflections and strains, and the very general time dependent inelastic behaviors which the basic theorem (Eqs. 15) is capable of treating. The calculations in such an approach will be long compared to those needed for small deflection problems, but since a statical problem must be treated by what is essentially a deformation theory of plasticity, they will be minor compared to those in wholly numerical complete solutions of the corresponding dynamic problems. The present method should provide guidance for such numerical solutions when complete time histories of response are required.

REFERENCES

1. A. R. S. Ponter, An Energy Theorem for Time Dependent Materials, *J. Mech. Phys. Solids* **17**, 63–71 (1969).
2. J. B. Martin, Impulsive Loading Theorems for Rigid–Plastic Continua, *J. Eng. Mech. Div. Proc. ASCE*, **EM5**, 27–42 (1964).
3. J. B. Martin, A Displacement Bound Principle for Inelastic Continua Subjected to Certain Classes of Dynamic Loading, *J. appl. Mech.* **32**, 1–6 (1965).
4. J. B. Martin, Extended Displacement Bound Theorems for Work Hardening Continua Subjected to Impulsive Loading, *Int. J. Solids Struct.* **2**, 9–26 (1966).
5. J. B. Martin, Displacement Bounds for Dynamically Loaded Elastic Structures, *J. Mech. Engng. Sci.* **10**, 213–218 (1968).
6. J. B. Martin and A. R. S. Ponter, Bounds for Impulsively Loaded Plastic Structures, *J. Eng. Mech. Div. Proc. ASCE*, **EM1**, 107–119 (1972).
7. J. B. Martin, Time and Displacement Bound Theorems for Viscous and Rigid–Viscoplastic Continua Subjected to Impulsive Loading, *Develop. Theoretical and App.. Mech.* **3**, 1–22 (1967).
8. J. B. Martin, The Determination of Upper Bounds on Displacements Resulting from Static and Dynamic Loading by the Application at Energy Methods, *Proc. Fifth U.S. Nat. Cong. Appl. Mech. ASME*, 221–236 (1966).
9. D. C. Drucker, A Definition of Stable Inelastic Material, *J. Appl. Mech.* **26**, 101–106 (1959).
10. D. C. Drucker, On the Postulate of Stability of Material in the Mechanics of Continua, *J. Mécanique* **3**, 235–249 (1964).
11. R. M. Haythornthwaite, Beams with Full End Fixity, *Engineering*, 110–112 (1957).
12. R. Hill, New Horizons in the Mechanics of Solids, *J. Mech. Phys. Solids* **5**, 66 (1956).
13. A. R. S. Ponter and J. B. Martin, Some Extremal Properties and Energy Theorems for Inelastic Materials and Their Relationship to the Deformation Theory of Plasticity, *J. Mech. Phys. Solids* **20**, 281–300 (1972).
14. P. S. Symonds and N. Jones, Impulsive Loading of Fully Clamped Beams with Finite Deflections and Strain-Rate Sensitivity, *Int. J. Mech. Sci.* **14**, 49–69 (1972).
15. P. S. Symonds, Survey of Methods of Analysis for Plastic Deformation of Structures under Dynamic Loading, Report BU/NSRDC/1-67, from Brown University to Office of Naval Research, Naval Ship Research and Development Center, Contract Nonr 3248(01)(X) (June, 1967).
16. B. Rawlings, Energy Absorption of Dynamically and Statically Tested Mild Steel Beams under Conditions of Gross Deformation, *Int. J. Mech. Sci.* **9**, 633–649 (1967).
17. R. J. Aspden and J. D. Campbell, The Effect of Loading Rate on the Elastic–Plastic Flexure of Steel Beams, *Proc. Roy, Soc.* **A290**, 266–285 (1966).
18. P. S. Symonds, Approximation Techniques for Impulsively Loaded Structures of Rate Sensitive Plastic Behavior, *SIAM J. appl. Math.* **25** (No. 3) (1973).
19. P. A. Symonds and T. J. Mentel, Impulsive Loading of Plastic Beams with Axial Constraints, *J. Mech. Phys. Solids* **6**, 186–202 (1958).
20. J. B. Martin and P. S. Symonds, Mode Approximations for Impulsively Loaded Rigid–Plastic Structures, *J. Eng. Mech. Div. Proc. ASCE* **92** (No. EM5), 43–66 (1966).
21. A. Nayfeh and W. Prager, On Martin's Lower Bound for Response Time of Impulsively Loaded Rigid–Plastic Structures, *ASCE Proc.* **95** (No. EM3), 813–819 (1969).

Note added in proof

It is implied by statements in the paper (e.g. page 422, sentence at end of lower paragraph) that no theorem is available furnishing an upper bound on the time t_f when deformation ceases. L. S. S. Lee [*J. Appl. mech.* **39**, 904–910 (1972)] has in fact stated and applied the following theorem: The deformation time t_f of the *mode form* solution with smallest rate of dissipation of energy, and whose initial kinetic energy is that of the impulsively loaded structure, is not less than that of the actual response of the structure. The method sketched in the present paper for determining an approximate upper bound on t_f, with consideration of finite deflections, will in many cases give a valid deflection bound, smaller than when Lee's theorem is used to obtain t_f. However, since it is not rigorous, it may be advisable also to make the calculation using t_f as computed by the theorem stated above. The authors are grateful to Dr. T. Wierzbicki for pointing out Lee's method.